ASTRONOMY & ASTROPHYSICS
SUPPLEMENT SERIES

*Astron. Astrophys. Suppl. Ser.* **126,** 357-364 (1997)



# Photometrically determined membership of the young, open cluster IC 2391

**W.R.J. Rolleston and P.B. Byrne**

Armagh Observatory, College Hill, Armagh BT61 9DG, N. Ireland

Received February 23, 1996; accepted March 20, 1997

**Abstract.** New 4-colour $BV(RI)_{\rm KC}$ CCD photometry to a limiting magnitude of $V \approx 19$ is presented for 1428 objects observed towards the direction of the young, open cluster IC 2391. We observed 36 ($2' \times 3'$) fields within 17 arcmin of the nominal cluster core. By fitting the theoretical isochrones of D'Antona & Mazzitelli (1994) to a combination of colour-magnitude and colour-colour diagrams, we have identified 17 stars as probable cluster members with a further 85 stars as possible members. The brightness distribution of low-mass members is compared with the luminosity function observed for the Pleiades and we estimate that the contamination due to background giants should be small.

**Key words:** stars: evolution — stars: late-type — open clusters: individual: IC 2391

## 1. Introduction

The pioneering work of Wilson (1963) and Kraft (1967) showed that stars of solar mass and less lose their angular momentum with time. Further research by van den Heuvel & Conti (1971) and Skumanich (1972) quantified the rate of loss. They considered both the strength of emission in the Ca II resonance lines as a proxy of stellar rotation (via magnetic field generation) as well as a small number of direct $v \sin i$ measurements of stars in three open clusters of increasing age, viz. the Pleiades, Ursa Major and the Hyades. These data along with similar measurements obtained for the Sun were used to show that stellar rotation decayed with age according to a power law with an index close to $-0.5$. This result was consistent with models of Durney (1972) in which rotational braking was caused by a stellar wind.

This wind-braking model became universally accepted for almost a decade and a half until it was challenged by the work of Stauffer et al. (1984, 1985, 1991a). These investigations involved the measurement of rotational $v \sin i$ for large numbers of GKM-type dwarfs in $\alpha$ Persei (age $\sim$ 50 Myr), the Pleiades (age $\sim$ 70 Myr) and the Hyades (age $\sim$ 800 Myr). Their results suggested that (a) rotational braking was mass dependent, ie. the more massive stars braking fastest, (b) that in the youngest clusters not all stars rotated rapidly and that many were rotating at a rate below the detection threshold of the data (20 km s$^{-1}$), and (c) that the time scale for braking the rotation of solar mass stars is comparable to, or even shorter than, the age difference between the $\alpha$ Per and Pleiades open clusters.

The fact that, even at the young age of the $\alpha$ Per system, many solar mass stars are slow rotators suggests that the initial distribution of angular momentum on the zero-age main-sequence is a function of the earlier evolutionary history of individual stars. For example, the interaction of the star with its environment during the late stages of contraction and the presence of circumstellar disks may play an important role (Li & Cameron 1993). Thus, the understanding of angular momentum evolution probably involves a detailed consideration of the interaction of stars with their environments and whether these include the formation of massive disks or not. It will also depend upon the validity of the assumption that each cluster can be taken as representative of clusters of that age in general.

Furthermore, it is apparent that the braking of the more massive fast rotators is extremely rapid. Any discussion of the timescales involved must inevitably take into account uncertainties in the cluster ages. For instance, in the case of $\alpha$ Per and the Pleiades, uncertainities in their ages are probably comparable to, or even larger than, their difference in age.

*Send offprint requests to*: W.R.J. Rolleston

[*] *Present address:* The Department of Pure and Applied Physics, The Queen's University of Belfast, Belfast BT7 1NN, N. Ireland.

[**] Figure 4 is only available in electronic form via http://www.ed-phys.fr.

Thus, it seems clear that further observations of a number of open clusters of various ages is vital in order to advance our understanding of the subject matter outlined above. The present authors have undertaken an observational programme of open clusters, both somewhat younger than $\alpha$ Per and between the ages of the Pleiades and Hyades, with a view to increasing the data available for this discussion. In our selection of clusters for investigation it is important to bear in mind the following considerations. In order that the measurement of $v \sin i$ will be feasible for individual stars (with presently available instrumentation), the study was restricted to clusters closer than ≈400 pc (ie. an M0 dwarf should be brighter than $V = 17.0$). However at such distances, open clusters have large extents on the sky resulting in a serious confusion between cluster stars and background objects. Hence, our programme should ideally consist of at least two steps, 1) the identification and elimination of background non-cluster members and then, 2) measurement of the rotational properties of resultant candidate members.

The first step may involve one or more of the following techniques, viz. multicolour photometry, proper motion studies, low-resolution spectroscopic classification and radial velocity measurements. This present paper is the first in a series identifying candidate members of appropriate young open clusters from the comparison of multicolour photometry and theoretical isochrones. A more detailed discussion of the points raised above has been given in Rolleston (1995).

## 2. IC 2391

IC 2391 is a young, nearby open cluster approximately centered on the bright star $o$ Velorum ($\alpha$=8$^{\rm h}$40$^{\rm m}$17.7$^{\rm s}$, $\delta$=−52°55′18″, J2000). Hogg (1960) and Lynga (1961) have obtained proper motions and photometry for the brighter members of this cluster, while spectroscopic data for these brighter members ($M_V \lesssim 4$) were presented by Feinstein (1961), Buscombe (1965), Perry & Bond (1969), Levato & Malaroda (1984) and Levato et al. (1988). These observations have shown that the cluster upper main-sequence contains approximately 22 members with spectral types earlier than mid-F. The apparent magnitudes and positions of these stars in the $(V, B-V)$ diagram are consistent with IC 2391 having a distance of order 150 pc and an age of order 3.6 $10^7$ yr. More recently, Stauffer et al. (1989) identified 10 late-type members with spectral types in the range G0V − M0V.

## 3. Observations

The photometric measurements were performed using the 1.0-m telescope at the South African Astronomical Observatory (SAAO) at Sutherland (Cape Province), during the period 15–22 January and 1-8 February 1994. An RCA CCD was employed which offers a detecting array of 320 × 512 pixels (Walker et al. 1984) and, combined with the available glass filters, this approximates to the Cousins $BV(RI)_{\rm KC}$ photometric system. At the Cassegrain focus a pixel (which is 27$\mu$m square) corresponds to 0.388 arcsec on the sky. We orientated the long axis of the CCD to be north-south and allowed for a 5 − 10% overlap between adjacent fields to assist with their registration, etc. This provided an effective non-overlapping image area of 2.0 × 3.0 arcmin of sky per frame. During this period, we imaged 36 fields in all four colours that were located around the core of the cluster. Care was taken to avoid fields that contained stars with magnitudes brighter than approximately $V = 9$, as it was found that the transfer of

**Table 1.** Coordinates of the field centres

| Id. | $\alpha$ (J2000.0) | $\delta$ (J2000.0) |
|---|---|---|
| 1 | 08 39 17.4 | −53 07 07 |
| 2 | 08 39 29.7 | −53 07 07 |
| 3 | 08 39 42.0 | −53 07 07 |
| 4 | 08 39 54.3 | −53 07 07 |
| 5 | 08 40 06.7 | −53 07 07 |
| 6 | 08 40 19.0 | −53 07 07 |
| 7 | 08 40 19.0 | −53 10 04 |
| 8 | 08 40 31.0 | −52 46 28 |
| 9 | 08 40 31.0 | −53 07 07 |
| 10 | 08 40 31.0 | −53 10 04 |
| 11 | 08 40 42.6 | −52 43 31 |
| 12 | 08 40 42.6 | −52 46 28 |
| 13 | 08 40 55.3 | −52 43 31 |
| 14 | 08 40 55.3 | −52 46 28 |
| 15 | 08 40 55.3 | −52 52 22 |
| 16 | 08 40 55.3 | −52 55 19 |
| 17 | 08 40 55.3 | −52 58 16 |
| 18 | 08 40 55.3 | −53 01 13 |
| 19 | 08 41 07.6 | −52 46 28 |
| 20 | 08 41 07.6 | −52 49 25 |
| 21 | 08 41 07.6 | −52 52 22 |
| 22 | 08 41 07.6 | −52 55 19 |
| 23 | 08 41 07.6 | −52 58 16 |
| 24 | 08 41 07.6 | −53 01 13 |
| 25 | 08 41 07.6 | −53 04 10 |
| 26 | 08 41 20.0 | −52 46 28 |
| 27 | 08 41 20.0 | −52 49 25 |
| 28 | 08 41 20.0 | −52 52 22 |
| 29 | 08 41 20.0 | −52 55 19 |
| 30 | 08 41 20.0 | −52 58 16 |
| 31 | 08 41 20.0 | −53 01 13 |
| 32 | 08 41 20.0 | −53 04 10 |
| 33 | 08 41 32.5 | −52 55 19 |
| 34 | 08 41 32.5 | −52 58 16 |
| 35 | 08 41 32.5 | −53 01 13 |
| 36 | 08 41 32.5 | −53 04 10 |

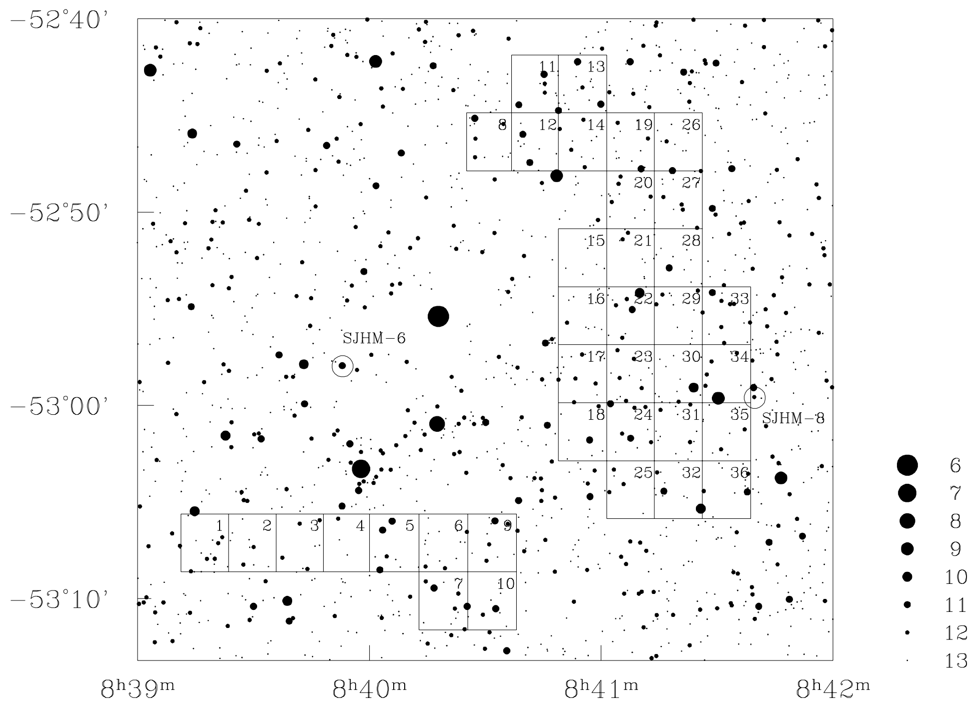


**Fig. 1.** A general view of the core of the open cluster, IC 2391, indicating those stars with visual magnitudes brighter than $V$=13.5. The area of sky imaged for each of the 36 fields is outlined by the boxes; the identification numbers corresponding to those given in Table 1. Cluster members previously identified by Stauffer et al. (1989) in this field are encircled and are labeled SHJM

excess charge from saturated objects along the geometry of the CCD precluded any useful photometric measurements. The coordinates of the field centres are presented in Table 1 and the area of sky that has been imaged is shown relative to the brightest stars in Fig. 1.

Typical exposure times were 600 : 300 : 120 : 120 seconds for the $B : V : R : I$ frames respectively. Fifteen E-region standard stars (Menzies et al. 1989) were observed for standardization purposes. These allowed an in-depth determination of the instrumental colour transformation to the standard system. In addition, 2–3 E-region stars were obtained throughout the night at similar air-masses to the programme fields for the determination of extinction coefficients and zero points. Furthermore, sky, flat, preflash and bias calibration frames were obtained at the beginning and end of each night.

## 4. Data reduction

The initial CCD reductions were performed using the CCDRED package within IRAF (Tody 1986). This procedure involved the replacement of bad pixels, subtraction of the mean overscan level, correction for any 2-dimensional structure in the bias level, trimming of the data section, subtraction of the preflash level and flat-fielding the CCD frames. Further details of this process can be found in Massey (1992).

**Table 2.** Transformation coefficients

| Filter | Coefficient | | | |
|---|---|---|---|---|
| | 1 | 2 | 3 | 4 |
| $b$ | 4.513 | −0.046 | 0.28 | −0.032 |
| $v$ | 4.449 | 0.018 | 0.15 | |
| $r$ | 4.123 | 0.006 | 0.13 | |
| $i$ | 4.908 | −0.049 | 0.11 | |

The stars were subsequently photometered using tasks within the IRAF package DAOPHOT (Davis 1994). Instrumental magnitudes for the standard stars were determined using digital aperture photometry, where for each night we have adopted an aperture radius to which all photometric measurements for that night are referred. This is essentially the same technique as used in standard photoelectric photometry. The choice of radius is governed by two opposing effects. Using as large an aperture as possible will include more starlight, however this will be accompanied by an increased sky contribution, as well as bad pixels and cosmic ray events. Although adopting a small aperture will provide the best signal-to-noise ratio, the results will not be consistent for different CCD frames as the effect of seeing and telescope focus will dominate the stellar profiles. Throughout the run, 2–3 arcsec seeing was

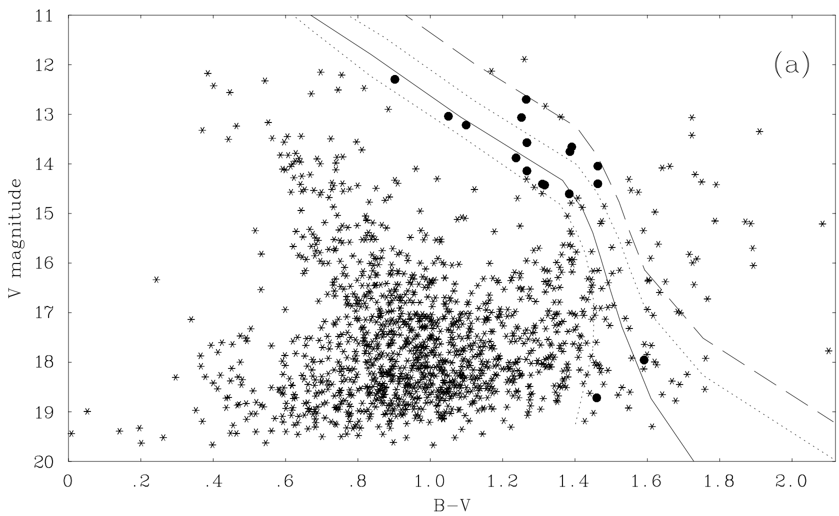


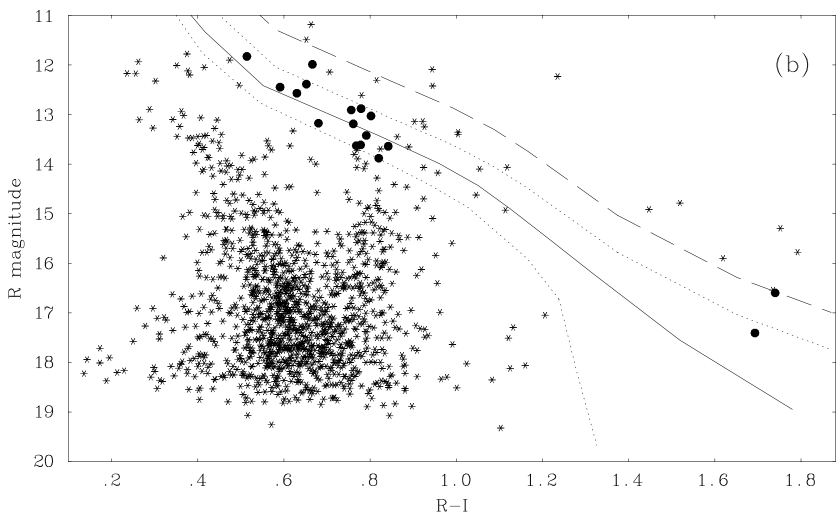


**Fig. 2. a)** The $(V,\ B-V)$ and **b)** $(R,\ R-I)$ colour-magnitude diagrams for the new photometric dataset. The solid line corresponds to the locus of a reddened 36 Myr isochrone and the dotted lines represent our estimates of upper and lower error limits for single stars having membership of IC 2391. The dashed line indicates the bright limit which accounts for the effect of binarity. Filled circles correspond to the candidate members identified using the selection criteria described in Sect. 5.3

typically encountered which corresponds to a stellar profile with a full-width-at-half-maximum (FWHM) of 5–8 pixels. As some 200 standard star observations were obtained, we investigated when the increase in starlight for larger apertures was masked by the photometric errors. We found that this occurred for a radius that was 6–7 times the FWHM of the stellar profile, and so a mean aperture was determined for each night's data.

Transformation equations of the form

$$b = B + b_1 + b_2(B-V) + b_3X + b_4(B-V)X$$
$$v = V + v_1 + v_2(B-V) + v_3X$$
$$r = R + r_1 + r_2(V-R) + r_3X$$
$$i = I + i_1 + i_2(V-I) + i_3X$$

were adopted, where $bvri$ are the instrumental magnitudes, $BVRI$ the standard magnitudes, $X$ the airmass and $b_1$ to $i_3$ are the transformation coefficients. The adopted zero points, colour terms and mean extinctions for the entire run were as given in Table 2.

Point-spread function photometry (PSF) was undertaken for the cluster fields, with independent PSF's being calculated for each CCD frame which were then used to derive instrumental magnitudes. An aperture correction was then applied to account for the smaller fitting radius

**Table 3.** Internal photometric errors as a function of brightness

| Magnitude range | $V$ | $B-V$ | $V-R$ | $V-I$ |
|---|---|---|---|---|
| $V \leq 13.0$ | 0.001 | 0.003 | 0.003 | 0.003 |
| $13.0-15.0$ | 0.003 | 0.005 | 0.005 | 0.005 |
| $15.0-17.0$ | 0.012 | 0.024 | 0.017 | 0.017 |
| $17.0-19.0$ | 0.056 | 0.112 | 0.077 | 0.080 |
| $V=19.0$ | 0.104 | 0.197 | 0.140 | 0.145 |

adopted in the PSF photometry compared to the large digital apertures used for the standard stars. IRAF estimates an internal error for these magnitudes which is based on the fitting procedure and in Table 3 we give the mean of these errors as a function of magnitude within each bandpass. Additionally, independent measurements of stars that were observed in the overlap region between adjacent fields were generally found to be consistent within the formal errors quoted in Table 3.

Photometry of all stars observed in this region of sky can be obtained electronically by ftp from the Centre de Données Stellaire, Strasbourg (130.79.128.5) or from the Armagh Observatory World Wide Web server (http://star.arm.ac.uk/) or by anonymous ftp upon request.

## 5. Discussion

### *5.1. Theoretical isochrones*

It is a standard technique to fit theoretical isochrones to the observed colour-magnitude diagrams and to select candidate cluster members from the relative positions of the stars in the former. An evolutionary age of 36 Myr has previously been determined for IC 2391 by applying this technique to the photometry of the early-type members. Assuming that coeval star formation has occurred, then many of the low-mass members will still be contracting towards the zero age main-sequence (ZAMS) and so it is important to use pre-main-sequence isochrones in any analysis. The most comprehensive and up-to-date computation of evolutionary tracks for low-mass stars ($M \leq 2.5\ M_{\odot}$) are those of D'Antona & Mazzitelli (1994). We have used the set of pre-main-sequence evolutions that have been modelled using the Alexander opacities (Alexander et al. 1989) and the mixing length treatment of Canuto & Mazzitelli (1990), as D'Antona & Mazzitelli have shown these to be in good agreement with observations of nearby M-dwarfs.

However, relating observed quantities such as $V, B-V$ and $R, R-I$ to the stellar parameters $\log L/L_{\odot}$ and $\log T_{\rm eff}$ is a non-trivial problem. Temperature calibrations have, in many instances, been determined for a particular range of spectral types and these different calibrations are not necessarily consistent. For example, Johnson (1966) derived a temperature calibration for early-type stars; Mould & Hyland (1976) for K-stars; Bessell (1991) for late-K to mid-M spectral types; and Reid & Gilmore (1984) for M-stars. In order to ensure some consistency, we have transformed the theoretical isochrones of D'Antona & Mazzitelli (1994) to observed colours and magnitudes as follows. For the late-K and M-stars ($0.53<(R-I)<2.38$), we have converted $T_{\rm eff}$ to $(R-I)$ and $M_{\rm bol}$ to $M_R$ using the revised relations of Bessell (1995). Additionally, the empirical relations of Caldwell et al. (1993) were used to transform $(R-I)$ colour to $(B-V)$. For the earlier spectral types (late-F to late-K), we used the theoretical colours and bolometric corrections of Kurucz computed by Wood & Bessell (private communication) and which are available via anonymous ftp from mso.anu.edu.au. This temperature calibration is quite similar to the IR flux method temperature scale of Blackwell & Lynas-Gray (1994).

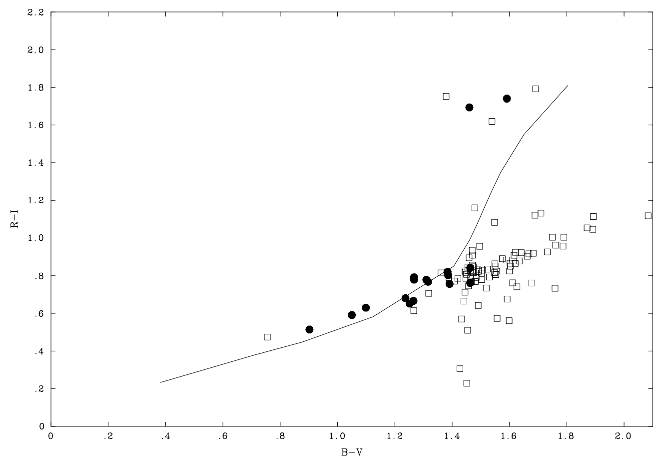


**Fig. 3.** The $(R-I, B-V)$ colour-colour diagram for the subset of stars that have been selected from the individual $(V, B-V)$ and $(R, R-I)$ CMDs using the criteria discussed in Sect. 5.3. Objects that satisfied both membership criteria are shown as filled circles. The solid line corresponds to the reddened 36 Myr isochrone

### *5.2. Observational errors*

In the photometric analysis we have assumed an evolutionary age of 36 Myr for IC 2391 (Lynga 1987) and a distance modulus, $(m-M)=6.05$, which has been derived using both photometric and spectroscopic techniques (Becker & Fenkart 1974). Adopting these values, we transformed a 36 Myr theoretical isochrone to fit the different combinations of CMDs and reddened these by the appropriate amount corresponding to a reddening value of $E(B-V)=0.04$ (Becker & Fenkart 1974).

In order to implement selection criteria for cluster membership, it is necessary however to consider the various sources of error in matching the observations to the theoretical isochrones. These include an uncertainty of

1. $\pm 10$ Myr in the cluster age, based on the dispersion of measurements found in the literature
2. $\pm 0.2$ magnitudes in the distance modulus (Becker & Fenkart 1974)
3. the magnitude dependent photometric uncertainties (see Table 3)
4. an error in the reddening value.

The slope of the pre-main-sequence isochrones and the reddening line in both the $(V, B-V)$ and $(R, R-I)$ CMDs is such that reddening serves to effectively move the isochrone to redder colour at all magnitudes for the colour range under consideration. As the reddening value of Becker & Fenkart has an uncertainty of $\pm 0.02$ magnitudes, we adopted an upper limit of $E(B-V) = 0.06$ for the bright error limits. However, for the faint error limits we have considered the possibility of negligible reddening and have adopted a value of $E(B-V) = 0.00$.

### *5.3. Cluster membership*

Candidate membership of the open cluster IC 2391 was based on the positions of stars in the $(V, B-V)$ and $(R, R-I)$ CMDs. We also consider the effect of binarity on the location of the theoretical isochrones (see, for example, Dabrowski & Beardsley 1977). Such an effect will obviously depend on the frequency of binaries and on the distribution of their mass ratios. However, assuming that an undetected companion has a lower mass and hence redder colour, its presence will cause its position to be shifted upwards in brightness and redwards in colour. Hence, the maximum increase in brightness allowing for a companion of equal mass would correspond to 0.75 magnitudes. This effect has been included in our bright error limit, and possible binary members were identified if they were situated between the single star, bright limit and the bright error limit. Objects were selected as possible members of IC 2391 if they were situated between the error limits as defined above. An object was then deemed a candidate member of IC 2391 if it fulfilled the selection criteria for *both* the $(V, B-V)$ and $(R, R-I)$ diagrams.

$BV(RI)_{\rm KC}$ CCD photometry was determined for 1303 objects in the field of IC 2391. Using the afore-mentioned selection criteria, 100 objects were identified as being possible cluster members, of which 83 satisfied the constraint for the $(V, B-V)$ CMD and 34 satisfied the constraint for the $(R, R-I)$ CMD respectively. A subset of these objects (16 of the 83 and 10 of the 34) were located within the binary envelopes of the respective CMDs. Seventeen objects satisfied both selection criteria and have been classified as candidate members; these exhibit a range of colours between approximately $0.4 \leq (R-I) \leq 1.7$ which corresponds to spectral types between G8V and M4V. Identification of main-sequence members of earlier spectral types was not possible, as these stars were saturated on the CCD frames. The photometry and sky charts for all 17 candidate members are presented in Table 4 and Fig. 4 respectively.

For a further 125 objects, it was only possible to determine two-colour photometry in either $BV$ or $RI$. In many cases, this was the consequence of their faintness and of the different limiting colour sensitivities. Additionally, some of the stellar profiles were severely contaminated by underlying bad pixels or cosmic ray events. However, two of these objects (1316 & 1428) were identified as having possible cluster membership (see Table 4).

The procedure discussed above for identifying cluster members is essentially the same as examining the $(R-I, B-V)$ colour-colour diagram (see Stauffer et al. 1989). In Fig. 3, we have plotted this diagram for the subset of stars that have been selected from the independent CMDs. It is clear that many of the stars with $B-V$ values redder than 1.5 and with $R-I$ values less than 1.2 can be excluded from further consideration. These objects probably correspond to the reddened background giant population. However, stars that have $B-V$ values bluer than 1.2 fall near the theoretical locus and even the two-colour diagram does not serve as a strong membership criterion. Hence, there may be a high contamination factor due to background objects in our candidate membership list. Unfortunately, due to the small image area of the RCA CCD, it would not have been observationally feasible to photometer a large number of offset fields in order to estimate the background contamination. Therefore, in the following section, we shall attempt to compare our results with the number density of low-mass objects found in the Pleiades.

### *5.4. Background contamination*

Although the total number of identified candidate members is small, it should be noted that approximately 25% of these objects are located within the limits for binarity, which is compatible with the binary frequency found in the Pleiades (Bettis 1975).

In recent years, many studies have been directed at the Pleiades in an attempt to determine the luminosity and mass functions (see, for example, Stauffer et al. 1991b; Hambly et al. 1991b; Schilbach et al. 1995). Unfortunately, this photometric study does not permit the construction of a luminosity function for IC 2391 (due to the small number of members that have been found). However, it is worthwhile to consider the luminosity function that is currently accepted for the Pleiades and to estimate what the total number of members to be expected in the area of sky (0.06 sq. degrees) that was photometered for IC 2391.

**Table 4.** Photometry of the candidate members

| Id. | $\alpha$ | $\delta$ | $V$ | $B-V$ | $V-R$ | $V-I$ |
|---|---|---|---|---|---|---|
| | (J2000.0) | | | | | |
| 162 | 08 40 05.68 | −53 05 59.971 | 13.065 | 1.252 | 0.677 | 1.329 |
| 302 | 08 40 31.18 | −53 11 44.415 | 14.605 | 1.384 | 0.724 | 1.544 |
| 311 | 08 40 32.50 | −53 10 32.571 | 12.295 | 0.902 | 0.466 | 0.980 |
| 314 | 08 40 32.99 | −53 10 29.804 | 13.217 | 1.099 | 0.646 | 1.276 |
| 348 | 08 40 38.40 | −53 06 29.594 | 14.405 | 1.310 | 0.792 | 1.570 |
| 362 | 08 40 39.75 | −52 45 58.903 | 12.700 | 1.265 | 0.711 | 1.377 |
| 448 | 08 40 52.26 | −52 46 46.917 | 14.426 | 1.316 | 0.798 | 1.566 |
| 480 | 08 40 53.89 | −52 42 14.523 | 14.142 | 1.267 | 0.719 | 1.510 |
| 581 | 08 40 59.89 | −52 44 27.479 | 13.752 | 1.386 | 0.722 | 1.524 |
| 586 | 08 40 59.99 | −52 44 21.420 | 13.572 | 1.267 | 0.691 | 1.470 |
| 711 | 08 41 06.96 | −52 51 04.148 | 13.880 | 1.237 | 0.705 | 1.385 |
| 729 | 08 41 08.02 | −53 00 04.475 | 17.955 | 1.591 | 1.357 | 3.097 |
| 872 | 08 41 15.40 | −53 00 14.300 | 13.040 | 1.050 | 0.591 | 1.182 |
| 950 | 08 41 18.30 | −52 47 52.839 | 14.045 | 1.463 | 0.856 | 1.617 |
| 955 | 08 41 18.65 | −52 58 54.409 | 18.718 | 1.460 | 1.312 | 3.005 |
| 1056 | 08 41 23.10 | −52 59 57.538 | 13.657 | 1.391 | 0.747 | 1.503 |
| 1144 | 08 41 26.57 | −53 04 26.286 | 14.401 | 1.463 | 0.760 | 1.602 |
| Id. | $\alpha$ | $\delta$ | $V$ | $B-V$ | | |
| 1316 | 08 40 25.78 | −53 11 15.093 | 18.654 | 1.641 | | |
| Id. | $\alpha$ | $\delta$ | $R$ | $R-I$ | | |
| 1428 | 08 41 39.62 | −52 59 34.208 | 12.613 | 0.780 | | |

Stauffer et al. (1991b) have identified 369 Pleiads in the magnitude range, $6 \leq M_V \leq 13$, distributed across 16 square degrees of sky. This magnitude range is similiar to that obtained in this study of IC 2391. As the Pleiades and IC 2391 open clusters have different distance moduli, we have applied a scaling factor in our calculation to account for the observed differences in their spatial extent. We have adopted angular diameters that have been based on the distribution of the early-type members in each cluster (Lynga 1987), and based on these observations made for the Pleiades field, approximately seven members are expected to be found in our sample for IC 2391.

However, Pleiads identified by Stauffer et al. (1991b) are distributed over a large area of sky, whereas our IC 2391 photometry has been obtained close to the cluster core where the star density may be expected to be greater. In fact, Hambly et al. (1991a) presented membership numbers as a function of radius which show that this scenario is true for the Pleiades. We have taken the star numbers for the inner 0.6° radius of the Pleiades, and estimate that approximately 24 members are to be expected in our sky sample, which is the same order of magnitude as the number of selected candidate members. These statistics would suggest that the background contamination of candidates is not severe. However, it should be noted that these estimates implicitly assume that both IC 2391 and the Pleiades have similar star densities and mass functions, an assumption which we can not comment further upon here.

### 5.5. Luminosity function

From an inspection of the CMDs (see Fig. 2), it would appear that very few members are to be found for spectral types later than M0V in IC 2391. This observation may be the result of having identified a small sample of candidate members and furthermore, a greater contamination of background objects may exist at GK-spectral types for the reasons discussed in Sect. 5.3. However, Foster et al. (1996) observed a sharp decline of cluster members in IC 2602 (age $\sim$ 20 Myr) at a spectral type of about M4v ($M_V \sim 11$). This dataset contained photometry of an offset field and this clearly showed that the selection criteria identified a significant excess number of stars in the cluster field compared with the former. Foster et al. were confident that the contamination of the selected possible members due to background objects was small, implying that this observed decline in the late-type members is real. Intermediate-resolution spectra of our candidates would enable us to obtain spectral classifications which, combined with the derived radial velocities, would permit confirmation of cluster membership.

Reid & Hawley (1996) have found a similar result in the old open cluster, M 67. In this case they have attributed the effect to dynamical "boiling-off" of the lower mass cluster members due to gravitational interaction of the cluster with passing massive objects. IC 2391, however, is too young for this mechanism to have operated.

### *5.6. Comparison with previous results*

Previously, only one investigation has been directed at the lower main-sequence of IC 2391. Stauffer et al. (1989) identified 10 GKM pre-main-sequence stars using both photometric and spectroscopic techniques. However, we did not obtain photometric measurements for any of these objects. This is a result of several factors. First, our brighter magnitude limit is ≈2 magnitudes fainter than that of Stauffer et al. Secondly, we avoided fields within several arcminutes of the bright stars ($V \leq 7$) as their reflected starlight contaminated the CCD frame, and thirdly, our sky coverage was severely curtailed by bad weather experienced throughout the run. Therefore, a direct comparison is not possible.

## 6. Conclusions

We have presented $BV(RI)_{\rm KC}$ CCD photometry of a 0.06 square degree near the nominal core of the open cluster, IC 2391. This data has been used to prepare $(V, B-V)$ and $(R, R-I)$ colour-magnitude diagrams. Superimposing theoretical isochrones appropriate to the age of IC 2391, we have identified 17 stars as candidate cluster members possessing colours and magnitudes corresponding to spectral types G8V − M4V. We have compared this number to the number of Pleiads that would be expected to be found in the same area of sky and deduce that, if the luminosity function and space distribution is similar to that of IC 2391, the contamination of our photometric candidate membership list by background objects should be small.

*Acknowledgements.* Research at Armagh Observatory is funded by a grant-in-aid from DENI. We would like to thank the staff of the South African Astronomical Observatory and Mr. Luis Sarro for their assistance in obtaining the observational data. Data reduction was performed on the PPARC funded Northern Ireland STARLINK node. WRJR acknowledges financial assistance from the PPARC, grant number GR/J25352.

## References

Alexander D.R., Augason G.C., Johnson H.R., 1993, ApJ 345, 1014
Becker J., Fenkart Q., 1974, ApJS 4, 240
Bessell M.S., 1991, AJ 101, 662
Bessell M.S., 1995, in The Bottom of the Main-Sequence ESO Workshop, Tinney C. (ed.). Garching, p. 123
Bettis C., 1975, PASP 87, 707
Blackwell D.E., Lynas-Gray A.E., 1994, A&A 282, 899
Buscombe W., 1965, MNRAS 129, 411
Caldwell J.A.R., Cousins A.W.J., Ahlers C.C., van Wamelen P., Maritz E.J., 1993, SAAO Circulars 15, 1
Canuto V.M., Mazzitelli I., 1990, ApJ 370, 295
Dabrowski J.P., Beardsley W.R., 1977, PASP 89, 225
D'Antona F., Mazzitelli I., 1994, ApJS 90, 467
Davis L.E., 1994, A Reference Guide to the IRAF/DAOPHOT Package, NOAO Laboratory
Durney B., 1972, NASA SP-308, 282
Feinstein A., 1961, PASP 73, 410
Foster D.C., Byrne P.B., Hawley S.L., 1996, A&A (submitted)
Hambly N.C., Jameson R.F., 1991a, MNRAS 249, 137
Hambly N.C., Hawkins M.R.S., Jameson R.F., 1991b, MNRAS 253, 1
Hogg A.R., 1960, PASP 72, 85
Johnson H.L., 1966, ARA&A 4, 193
Kraft R.P., 1967, ApJ 150, 551
Levato H., Malaroda S., 1984, ApJ 24, 37
Levato H., García B., Loustó C., Morrell N., 1988, Ap&SS 146, 361
Li J., Cameron A.C., 1993, MNRAS 261, 766
Lynga G., 1987, in Catalogue of Open Cluster Data, CDS, Strasbourg
Lynga G., 1961, Ark Astr 34, 379
Massey P., 1992, A User's Guide to CCD Reductions with IRAF, NOAO Laboratory
Menzies J.W., Cousins A.W.J., Banfield R.M., Laing J.D., 1989, SAAO Circulars 13, 1
Mould J.R., Hyland A.R., 1976, ApJ 208, 399
Perry C.L., Bond H.E., 1969, PASP 81, 629
Reid N., Gilmore G., 1984, MNRAS 206, 19
Reid I.N., Hawley S.L., 1996, in Cool Stars, Stellar Systems and the Sun, 9$^{\rm th}$ Cambridge Workshop (in press)
Rolleston W.R.J., 1995, Ir. Astron. J. 22, 181
Schilbach E., Robichon N., Souchay J., Guibert J., 1995, A&A 299, 696
Skumanich A., 1972, ApJ 171, 565
Stauffer J.R., Hartmann L., Soderblom D.R., Burnham N., 1984, ApJ 280, 202
Stauffer J.R., Hartmann L., Burnham N., Jones B.F., 1985, ApJ 289, 247
Stauffer J.R., Hartmann L., Jones B.F., McNamara B.R., 1989, ApJ 342, 285
Stauffer J.R., Giampapa M.S., Herbst W., et al., 1991a, ApJ 374, 142
Stauffer J.R., Klemola A., Prosser C., Probst R., 1991b, AJ 101, 980
Tody D., 1986, IRAF User Manual, NOAO Laboratory
van den Heuvel E.J., Conti P., 1971, Sci. 171, 895
Walker D., Walker A., Sanford P., 1984, Proc. 8$^{\rm th}$ on Photoelectric Imaging Devices
Wilson O.C., 1963, ApJ 138, 832